Proceedings of the ASME 2009 Dynamic Systems and Control Conference
DSCC2009
October 12-14, 2009, Hollywood, California, USA

DSCC2009-2614

CONTROL-ORIENTED MODELING OF A SOLID-OXIDE FUEL CELL STACK USING AN LPV MODEL STRUCTURE

Borhan M. Sanandaji, Tyrone L. Vincent*, Andrew Colclasure, and Robert J. Kee

Colorado Fuel Cell Center
Engineering Division
Colorado School of Mines
Golden, CO 80401
Email: {bmolazem,tvincent,acolclas,rjkee}@mines.edu

ABSTRACT

For efficient operation, as well as to avoid operating conditions that can cause damage, fuel cells require a control system to balance fuel and air supply and electrical load. The need to maintain signal constraints during operation, combined with importance of unmeasured variables such as internal stack temperature or fuel utilization, indicate the need for control-oriented models that can be used for estimation and model predictive control. In this paper, we discuss the development of a control-oriented dynamic model of a solid oxide fuel cell stack. Using a detailed physical model as a starting point, we demonstrate the utility of a linear parameter varying (LPV) model structure as a mechanism for model reduction. A novel feature is a non-parametric method for determining the scheduling functions in this model.

INTRODUCTION

Fuel cells are devices that enable the direct conversion of chemical energy into electrical energy, with a theoretical conversion efficiency much higher than for heat engines [1, 2]. The main component of a cell is a anode/electrolyte/cathode structure, which is exposed to fuel on the anode side and an oxidant (usually air) on the cathode side. Solid-oxide fuel cells (SOFCs) utilize a ceramic oxygen-ion conducting electrolyte. Oxygen ions are formed at the cathode, which migrate through the electrode. At the anode, these ions react with hydrogen and carbon monoxide to produce water and carbon dioxide, as well as releasing electrons that flow through an external circuit back to the cathode. A particular characteristic of SOFC fuel cells is their ability to operate on hydrocarbon fuels with either internal or external reforming, eliminating the need for hydrogen storage.

To operate at multiple power levels, fuel cells require a control system to balance the fuel and air supply, as well as the electrical load. This is important both to achieve high efficiency, as well as to avoid operating conditions that can damage the fuel cell, such as excessive temperature or temperature gradients [3], coking [1], and anode reoxidation [4]. Because of these important operating limits, as well as the strong interaction between input variables, model predictive control (MPC) is a natural choice for control implementation.

However, to implement model predictive control, a control-oriented model is needed that captures the dominant input-output behavior. One way to develop such a model is a physics-based component model using flow characteristics, lumped-volume manifold filling dynamics, simplified electrochemistry, and simple diffusion, transport, and heat equations. Such a control-oriented modeling of proton exchange membrane (PEM) fuel cells has been explored in [5] and for SOFCs in [6]. However, when choosing which physical effects to include, it is often difficult to balance simplicity with fidelity. Another way to obtain a control-oriented model is to fit low order empirical model structures to experimental data, and this has been utilized for PEM fuel cells in [7, 8]. However, this approach fails when there are important model variables (such as internal temperatures or fuel utilization) that cannot be measured.

An alternative approach is to start with a high order physically-based model, and use model reduction to obtain a control-oriented model. This control-oriented model will have a low number of states but capture the dominant system dynamics accurately over a range of frequencies and operating points. In

*Address all correspondence to this author.

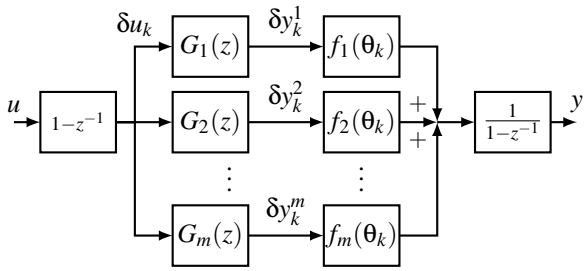

Figure 1: LPV MODEL STRUCTURE FOR LOW ORDER REPRESENTATION.

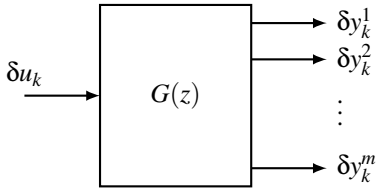

Figure 2: COMBINED LINEAR MODEL FOR SMALL SIGNAL BEHAVIOR AT MULTIPLE SETPOINTS.

this paper, we develop a control-oriented model of an SOFC fuel cell stack via the use of a linear parameter varying (LPV) model structure. The model reduction proceeds in two steps. In the first step, a set of operating points are selected and linear models are obtained which model the small signal behavior. The linear models are combined and the redundant modes eliminated via linear model reduction. This is followed by a second step in which nonlinear functions are identified that modulate the outputs of the small signal models in a manner similar to gain scheduling. A particular contribution of this paper is a novel non-parametric approach for identifying the scheduling functions.

MODEL REDUCTION USING LPV MODEL STRUCTURE

The LPV model structure is shown in Fig. 1, where z is the forward shift operator. The linear systems $G_i(z)$ capture small signal behavior at m different operating points. The variable θ is a scheduling parameter that is a function of the (measured) system output, and $f_i(\theta)$ represent gains that are nonlinear functions of θ. Since each of the linear models captures only small signal behavior, the operating point needs to be removed at the input, and added back at the output. This is accomplished by applying a first difference $(1-z^{-1})$ of the input, and integrating $\left(\frac{1}{1-z^{-1}}\right)$ the the outputs. Below, we describe methods to estimate the linear models ($G_i(z)$) and parameter varying ($f_i(\theta_k)$) portions of the model. We will describe later a simple estimation method to adjust for accumulated errors in the integral states.

Identification of linear part

Although linearization followed by balanced model reduction and conversion to discrete time is the typical path to obtain a small signal reduced order model, we have chosen to use a data based method instead, based on the subspace class of system identification methods. In essence, we treat the model as an experiment, albeit one without measurement noise. This has several distinct advantage. First, there is no need for the physical model to be in a standard form. For example, in our case, the physical model is expressed in the form of a differential-algebraic equations (DAE), rather than ordinary differential equations (ODE). The linearized model would then be of DAE form, complicating the subsequent model reduction. Secondly, a data-based model will be close to the best linear approximation of the nonlinear system as measured over the amplitude and frequency range of the experimental input, whereas a linearized model has no corresponding approximation qualities.

The data collection proceeds as follows. A set of operating points $(\bar{u}^i, \bar{y}^i)$, $i = 1, \ldots, m$, are chosen that span the desired operating range. A small signal input sequence δu is designed with frequency content that matches the expected system bandwidth. This input is applied at each operating point $u = \bar{u}^i + \delta u^i$, and the small signal response $\delta y^i = y - \bar{y}^i$ is recorded.

From this data, reduced order models of the small signal behavior are identified. In order to take advantage of possible repeated modes between operating points, we will combine the small signal models into a single model, as shown in Fig. 2. Thus, in what follows, we will take the output of the identified system as $\delta y = \begin{bmatrix} \delta y^1 & \delta y^2 & \cdots & \delta y^m \end{bmatrix}$.

Our method to fit a low order model to the data comes from the subspace identification methods (see e.g. [9]), and is briefly summarized here. Given a collection of input/output measurements $(\delta u_k, \delta y_k)$, $k = 1, \cdots, N$, we wish to find a linear time invariant (LTI) system in state space form,

$$\begin{cases} x_{k+1} = \Phi x_k + \Gamma \delta u_k \\ \delta y_k = C x_k + D \delta u_k \end{cases}, \tag{1}$$

that can closely reproduce this data, where $x_k \in R^n$ is the state vector, and all other vectors/matrices are assumed to have compatible dimensions. To find the parameters of this model (Φ, Γ, C, D), we note that if Eq. (1) did generate this data, then we could write

$$Y_s = \Gamma_s X + H_s U_s, \tag{2}$$

where

$$Y_s = \begin{bmatrix} \delta y_1 & \dots & \delta y_{N-s+1} \\ \vdots & \vdots & \vdots \\ \delta y_s & \dots & \delta y_N \end{bmatrix},$$
$$U_s = \begin{bmatrix} \delta u_1 & \dots & \delta u_{N-s+1} \\ \vdots & \vdots & \vdots \\ \delta u_s & \dots & \delta u_N \end{bmatrix},$$
$$X = [x_1\ x_2\ \dots\ x_{N-s+1}],$$

and

$$H_s = \begin{bmatrix} D & 0 & \cdots & 0 \\ C\Gamma & D & \ddots & \vdots \\ \vdots & & \ddots & 0 \\ C\Phi^{s-1}\Gamma & \cdots & C\Gamma & D \end{bmatrix}, \quad \Gamma_s = \begin{bmatrix} C \\ C\Phi \\ \vdots \\ C\Phi^s \end{bmatrix}.$$

The system parameters are contained in H_s and Γ_s, and could be extracted if these terms were known. Note that in Eq. (2), matrices Y_s and U_s are known from the measurements. We can remove the H_sU_s term by multiplying it by its orthogonal complement ${\Pi_{U_s^T}}^{\perp}$ as follows:

1. Form ${\Pi_{U_s^T}}^{\perp} = I - U_s^T(U_sU_s^T)^{-1}U_s$ (Note that $U_s{\Pi_{U_s^T}}^{\perp} = U_s - \underbrace{U_sU_s^T(U_sU_s^T)^{-1}}_{\text{unity matrix}}U_s = 0$)
2. Multiply Eq. (2) from right by ${\Pi_{U_s^T}}^{\perp}$ to give

$$Y_s{\Pi_{U_s^T}}^{\perp} = \Gamma_s X{\Pi_{U_s^T}}^{\perp}.$$

Since Γ_s is a rank n matrix, we can apply the singular value decomposition (SVD) to $Y_s{\Pi_{U_s^T}}^{\perp}$ to find S and V orthonormal and Σ diagonal such that

$$Y_s{\Pi_{U_s^T}}^{\perp} = S\Sigma V^T. \tag{3}$$

An estimate for Γ_s is then taken as the n first columns of S. (Note that Γ_s is defined only within a coordinate transformation of x_k.) With Γ_s known, we can find C as the first rows of Γ_s, and then determine Φ through the shift pattern of Γ_s. With Φ and C in hand, Γ and D are linear in Eq. (2) and can be found via linear least squares.

Identification of scheduling functions

From the results of the previous section, we have available the small signal models $G_i(z)$ for m different operating points. Thus, each system $G_i(z)$ models the small signal behavior for one value of the scheduling parameter θ. Let ϕ^i be the value of θ that corresponds to the operating point for system $G_i(z)$. In this section, we describe how the scheduling functions $f_i(\theta)$ are selected to match the system response to a large signal experiment. This experiment must perturb the model's inputs with signals of sufficiently large variation that during the experiment the system moves across all operating points.

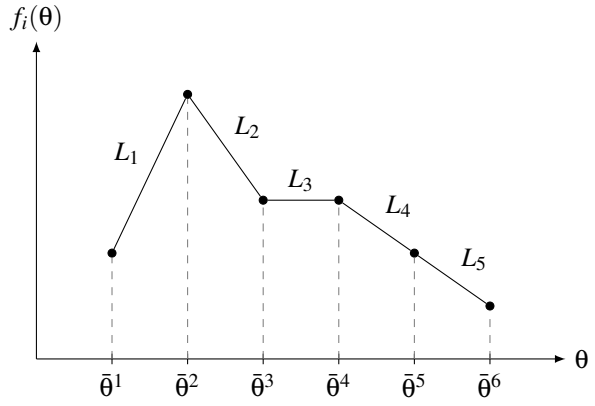

Figure 3: SCHEDULING FUNCTION $f_i(\theta)$

Rather than using a parameterized basis expansion of $f_i(\theta)$, the estimate of $f_i(\theta)$ will be found directly in terms of the function values. Specifically, the scheduling parameter θ is quantized into a fixed number of "bins" with centers $\bar{\theta}^j$, $j = 1,\dots,\ell$, and our objective will be to estimate the values for $f_i(\bar{\theta}^j)$ for all i, j as shown in Fig. 3. In other words, the set of values $f_i(\bar{\theta}^j)$ for all i, j become the parameters to be identified. Note that the ℓ can be much larger than m. Once these values have been found, the functions $f_i(\theta)$ could be represented by an appropriate interpolation of these points. Given a measured scheduling sequence θ_k, let $\bar{\theta}_k$ be the quantized scheduling sequence, such that for all k, $\bar{\theta}_k = \bar{\theta}^j$ for some j, and $\|\theta_k - \bar{\theta}_k\|$ is minimized, where $\|\cdot\|$ is the Euclidean norm.

Since $G_i(z)$ is known, the signals

$$\delta y_k^i = G_i(z)(1 - z^{-1})u_k$$

can be calculated, where u_k is the input used in the experiment. The output y_k and quantized scheduling sequence $\bar{\theta}_k$ for this experiment are also known. Our objective is to select the values of $f_i(\bar{\theta}^j)$ such that $\delta y_k \approx \delta\hat{y}_k$, where δy_k is the first difference of the measured output

$$\delta y_k = (1 - z^{-1})y_k, \tag{4}$$

and

$$\delta\hat{y}_k = \sum_{i=1}^{m} f_i(\bar{\theta}_k)\delta y_k^i. \tag{5}$$

Clearly, without placing restrictions on $f_i(\bar{\theta}^j)$, this problem is under-determined. One set of constraints on the scheduling functions come from their definition: they should range from 0 to 1, and the sum of the scheduling functions over i for any $\bar{\theta}^j$ should always add to one. In addition, we require that the functions be sufficiently smooth, where as a measure of smoothness, we use the *dispersion function* which was introduced in [10] for nonparametric identification of nonlinear systems. The dispersion function is a smoothness measure for functions that are described point-wise, and is closely related to total variation. As described in [10], it can be extended to multi-dimensional functions, but for simplicity we will restrict to scalar $\bar{\theta}$ here. Given a point-wise description of a function in terms of points $(\bar{\theta}^j, f(\bar{\theta}^j))$, let

$$\mathcal{D}(f(\bar{\theta}^j)) = \sum_{j=1}^{\ell-1} L_j^2$$

be the dispersion of f, where L_j are the lengths of a linear interplant of $(\bar{\theta}^j, f(\bar{\theta}^j)$, as shown in Fig. 3. Note that the dispersion is a quadratic function of the values of $f(\bar{\theta}^j)$.

By solving the following optimization problem, we find the values of the scheduling functions $f_i(\bar{\theta}^j)$ for all i, j that minimize a weighted sum of the fit error and the dispersion, subject to the constraints.

$$\begin{array}{cc} \min_{f_i(\bar{\theta}^j)} & \sum_{k=1}^{N} \|\delta y_k - \delta \hat{y}_k\|^2 + \beta \sum_{i=1}^{m} \mathcal{D}(f_i(\bar{\theta}^j)) \\ \text{subject to} & 0 \le f_i(\bar{\theta}^j) \le 1 \\ & \sum_{i=1}^{m} f_i(\bar{\theta}^j) = 1 \\ & f_i(\phi^j) = 1 \end{array} \tag{6}$$

where β is a user-defined parameter. Since the dispersion is a quadratic function of $f_i(\bar{\theta}^j)$, this is a convex optimization problem, and can be easily solved using modern optimization packages as a second order cone problem.

SOFC STACK MODEL

In this section, we discuss the detailed physical model of the SOFC stack which is to be reduced using LPV model structure.

Solid oxide fuel cells (SOFC) can be operated with a variety of fuels, including hydrogen, CO, hydrocarbons, or mixtures of these. This is possible because of the relatively high operating temperatures, $(600 - 800\,^{\circ}\mathrm{C})$, and, at least in conventional SOFC anodes, the use of transition metal catalysts that promote the water-gas-shift (WGS) reaction as in Eq. (7):

$$\mathrm{CO} + \mathrm{H_2O} \rightleftharpoons \mathrm{CO_2} + \mathrm{H_2} \tag{7}$$

and steam reforming, which for methane may be written globally as Eq. (8):

$$\mathrm{CH_4} + \mathrm{H_2O} \rightleftharpoons \mathrm{CO} + 3\mathrm{H_2} \tag{8}$$

If sufficient steam is produced electrochemically at the anode/-electrolyte interface by the reaction as in Eq. (9):

$$\mathrm{H_2} + \mathrm{O^{2-}} \rightleftharpoons \mathrm{H_2O} + 2\mathrm{e^-} \tag{9}$$

then reforming and shifting can, in principle, lead to full (if indirect) electrochemical oxidation of a hydrocarbon fuel [11].

Figure 4 illustrates the nominal geometry for an anode-supported tubular cell [12]. The central component of a cell is the membrane-electrode assembly (MEA), which consists of an electrolyte sandwiched between an anode and a cathode. The electrolytes are oxygen-ion conductors but are impervious to gas flow and have negligible electronic conductivity. The anode is the electrode on the fuel side and the cathode on the air side. The electrodes must be electronic conductors and may also serve as a catalyst or electro catalyst. As illustrated in Fig. 4, the anode and cathode are connected by an external circuit [12].

SOFCs involve complex physicochemical processes. Oxygen is electrochemically reduced at the cathode-electrolyte-air three-phase boundary (TPB). In global terms, electrons from the cathode react with oxygen molecules in the air to deliver oxygen ions into the electrolyte via a charge-transfer reaction:

$$\mathrm{O_2(g)} + 4\mathrm{e^-(c)} \rightleftharpoons 2\mathrm{O^{2-}(e)} \tag{10}$$

The three phases are denoted as (g) for the gas, (c) for the cathode, and (e) for the electrolyte. Oxygen ions migrate through the electrolyte via a vacancy hopping mechanism toward the anode-electrolyte-fuel TPB, whereupon they can participate in the electrochemical oxidation of fuels. For example, a global H_2 oxidation may be written as in Eq. (11):

$$\mathrm{H_2(g)} + \mathrm{O^{2-}(e)} \rightleftharpoons \mathrm{H_2O(g)} + 2\mathrm{e^-(a)} \tag{11}$$

where the gas-phase H_2 reacts with the O_2 from the electrolyte to produce steam in the gas phase and deliver electrons into the anode. As long as a load is connected between the anode and cathode, the electrons from the anode will flow through the load back to the cathode, therefore, electric current, i, will flow through the circuit as shown in Fig. 4. By convention, the direction of electric current, i, is opposite to that of the electron flow.

Model Development

The high order fuel cell model uses the differential algebraic equation solver IDA to solve time dependent conservation equations for the fuel channel flow, porous-media transport, MEA temperature, heterogeneous chemistry, and electrochemistry. Fuel channel flow is modeled with a series of perfectly stirred reactors. Species fluxes within the anode are calculated using the Dusty Gas Model. Heterogeneous chemistry inside the anode is modeled with global reactions for steam reforming and

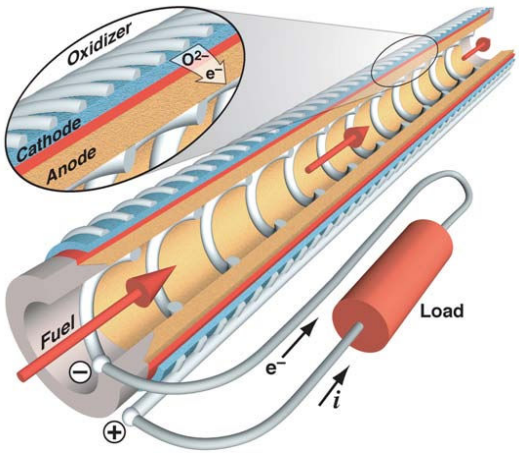

Figure 4: SKETCH OF AN ANODE-SUPPORTED TUBULAR SOFC

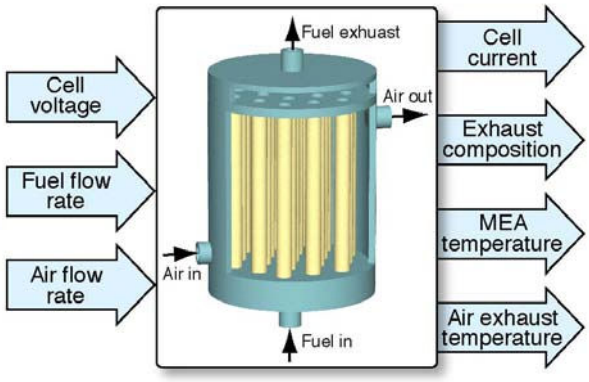

Figure 5: SOFC BLOCK DIAGRAM

the water-gas-shift reaction. Modified Butler-Volmer equations describe the electrochemistry occurring at the cathode and anode triple phase boundaries. The model neglects cathode gas composition variations because the cathode is very thin in comparison to the anode. Due to significant mixing, the air flow is modeled with a single perfectly stirred reactor [11].

The fuel cell model is based on an anode supported tube consisting of a Ni-YSZ anode, YSZ electrolyte, and LSM-YSZ cathode. The fuel channel inlet consists of an equilibrium mixture of methane and air at 800°C with an Oxygen-to-Carbon ratio of 0.5. The model captures flow and thermal dynamics, which are on the order of seconds and hundreds of seconds, respectively. Flow response consists of gas diffusion through the anode and gas flow through the fuel channel. The heat capacity of the tube and air flow controls the thermal response. The only dynamic not captured is the double layer charging between metal and ceramic particles. This dynamic is assumed to be negligible because the characteristic time is on the order of milliseconds.

For system identification and control purposes, we consider the solid-oxide fuel cell (SOFC) stack as a system with three inputs and four outputs, as shown in Fig. 5. We consider an ideal stack where all of the tubes have the exact same conditions. Thus, a tube model is developed for a single anode-supported tube with fuel flowing through the inside of the tube and air blowing around the outside. Stack power and flow rates are found by taking results from the tube model and multiplying by the number of tubes.

RESULTS

In this section, we explain the steps used to identify a multi-input multi-output (MIMO) SOFC stack model.

We consider 3 inputs and 4 outputs for the SOFC stack model. The inputs are Fuel Flow Rate (Kg/s), Cell Voltage (volts), and Air Flow Rate (Kg/s). The outputs are Current (amps), Hydrogen Concentration in Fuel Flow Exhaust (mole fraction), Average MEA Temperature (Kelvin) and Temperature of Air Flow Exhaust (Kelvin). The block diagram of the SOFC stack is shown in Fig. 5.

From preliminary step experiments, we find that there is a large difference in the time constants associated with system outputs. The current output has the smallest time constant and is of the order of a fraction of a second. However, Hydrogen concentration and output temperatures have much larger time constants. Time constant for Hydrogen concentration is of the order of $4-5$ seconds and for output temperatures is of the order of minutes. Therefore, the initial small signal experiments need to perturb the system inputs over three different frequency bands.

The model is interrogated with test signals which are suitable for model identification. These test signals have two important aspects, the first is the shape or waveform of the signal and the second is its power spectrum or frequency content. These test signals are added to the manipulated inputs (MPs) of the open-loop process in order to move the process up and down around a working/operating point, therefore, the mean value of the test signals should be zero or close to zero. Among different types of test signals, the pseudo-random-binary-sequence (PRBS) is one of the most popular ones [13]. This is called a pseudo-random because it is a deterministic signal yet its autocorrelation function can resemble the autocorrelation function of a white random noise with zero mean.

Because the dominant system's time constants can be separated between the electrical, exhaust composition, and thermal outputs, the small signal identification can be approached as the identification of three different systems: one with current, one with exhaust composition, and one with MEA and exhaust temperatures as the outputs. Three different experiments were performed, with the sampling times (i.e. PRBS time constant) chosen as $T_s = 0.0125$ (s) for the current system, $T_s = 0.125$ (s) for the composition system, and $T_s = 1.25$ (s) for the temperatures system. An experiment of 500 samples was performed in each case, with each input perturbed sequentially. Sequential pertur-

Table 1: OPERATING POINTS ASSOCIATED WITH SMALL SIGNAL MODELS.

	OP1	OP2	OP3	OP4
Voltage (v)	0.65	0.70	0.75	0.80
Air Flow (g/s)	0.335	0.335	0.335	0.335
Fuel Flow (g/s)	0.0445	0.0445	0.0445	0.0445
Current (A)	28.64	26.75	22.34	16.95
H_2 Mole Fraction	0.0080	0.0305	.0909	0.1676
MEA Temp. (K)	1111	1104	1094	1085
Air Temp. (K)	1081	1079	1075	1071

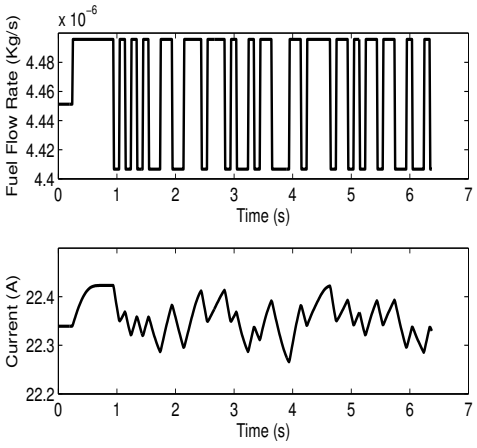

Figure 6: SMALL SIGNAL EXPERIMENT WITH FUEL FLOW PERTURBATION AND CURRENT RESPONSE

bation is used to facilitate normalization of signals sizes before applying the subspace identification procedure.

In these experiments, we consider four operating points, which are listed in Tab. 1. A short segment of an experiment at the first operating point (OP1) is shown in Fig. 6. In this segment, the fuel flow rate is perturbed while the other inputs are held constant at their nominal operating values. The upper plot shows PRBS signal that is applied to the fuel flow rate. The lower plot is the response of the current. In what follows, we will concentrate on the results for the current output.

Using the resulting experimental data from the model, we are able to identify the the combined reduced order model of the SOFC stack model at four different operating points using subspace identification method discussed earlier. Based on a comparison of the model fit, a model size of 8 states was chosen for each 3×1 or 3×2 subsystem.

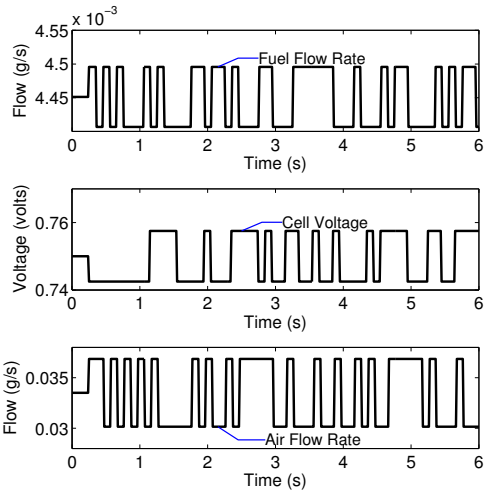

Figure 7: PERTURBATION INPUTS FOR SMALL SIGNAL MODEL VALIDATION

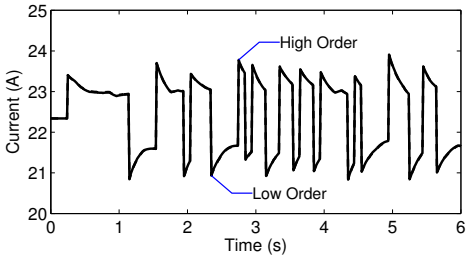

Figure 8: COMPARISON OF HIGH ORDER AND LOW ORDER MODEL FOR VALIDATION EXPERIMENT

To validate these small signal models, a second perturbation sequence was used, which is shown in Fig. 7. A comparison between the high order physics based model and the low order small signal model for operating point OP1 is shown in Fig. 8. Note that the two curves are indistinguishable.

Gain Scheduling

As scheduling parameter, we chose the output current. In order to transit between different operating points, we perturb cell voltage system input with a large signal change as is shown in Fig. 9. Solving the optimization problem as described in Eq. (6), we are able to identify 4 scheduling functions corresponding to 4 operating points. These functions are shown in Fig. 10.

Figure 11 shows the estimated output current versus desired (driven from high order SOFC stack model) output current. As it can be seen, the LPV scheme which is based on small signal transfer functions can estimate the output pretty well. However, the estimated output seems to start drifting from the desired out-

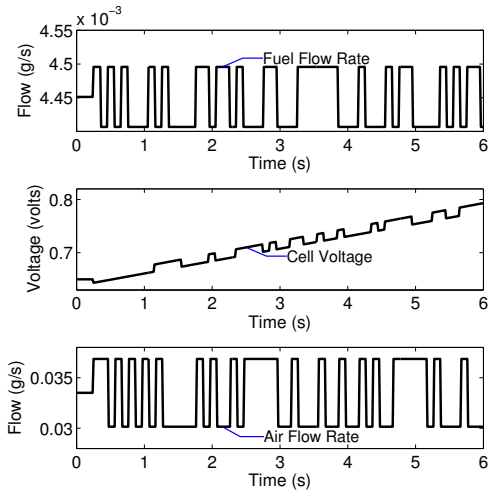

Figure 9: PERTURBATION EXPERIMENT WITH LARGE SCALE VARIATION IN VOLTAGE

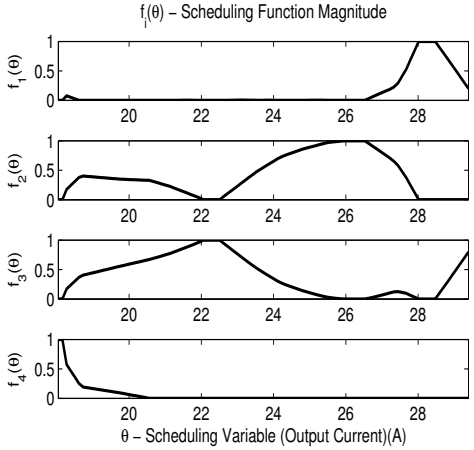

Figure 10: IDENTIFIED SCHEDULING FUNCTIONS

put after passing some time. This is because of error accumulation in the integrator and can be corrected significantly by adding a simple predictor to the LPV scheme.

The integrator is modified by the addition of a simple error correction term as follows

$$\hat{y}_k = \hat{y}_{k-1} + \delta\hat{y}_k + k(y_{k-1} - \hat{y}_{k-1}) \tag{12}$$

where $\hat{y}$ is the output of the LPV model, and y_k is the output of the actual system. Since this model is intended to be used online during control, the value of the system output y_{k-1} will be available for use.

As it can be seen from Eq. 12, the prediction parameter, k, is a free parameter, which we chose to be .01. The effect of adding this drift correction is shown in Fig. 12

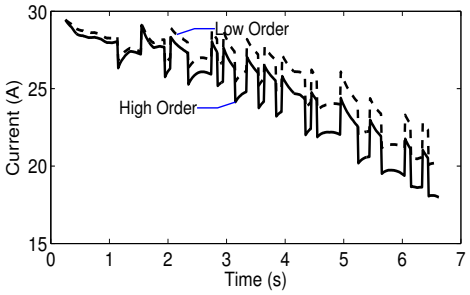

Figure 11: REDUCED vs. FULL ORDER MODEL CURRENT OUTPUT

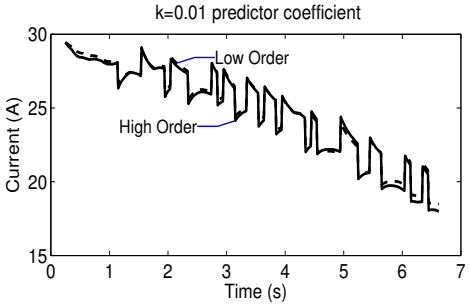

Figure 12: REDUCED vs. FULL ORDER MODEL CURRENT OUTPUT WITH PREDICTOR

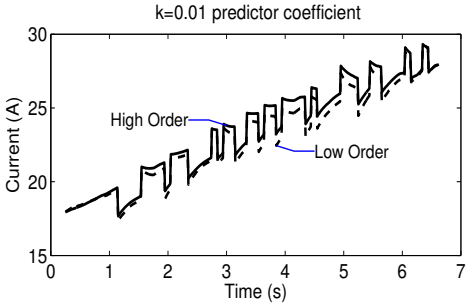

Figure 13: REDUCED vs. FULL ORDER MODEL CURRENT OUTPUT (VALIDATION)

In order to validate the scheduling functions we identified, we perform another experiment to get a new data set for validation. In this experiment we linearly decrease the input cell voltage from 0.80 (volts) down to 0.65 (volts). The output estimate is shown in Fig. 13. We see that the fit between reduced and full order model is quite good.

CONCLUSION

In this paper, we have explored the use of a LPV model structure as a mechanism for model reduction of a detailed physical model of an SOFC fuel cell stack.

These preliminary results have only utilized output current as a scheduling parameter, however, it expected that both current and cell temperature will need to be utilized to determine operating point. In addition, in the large scale experiment, only the cell voltage was perturbed over a wide range. These deficits are being addressed in the work currently underway.

ACKNOWLEDGMENT

This work has been funded in part by the Department of Energy, Office of Energy Efficiency and Renewable Energy, Contract Number DE-FG36-08GO88100.

REFERENCES

[1] Kee, R. J., Zhu, H., and Goodwin, D. G., 2005. "Solid-oxide fuel cells with hydrocarbon fuels". *Proceedings of the Combustion Institute,* **30**, pp. 2379–2404.

[2] Kee, R., Zhu, H., Sukeshini, A., and Jackson, G., 2008. "Solid oxide fuel cells: Operating principles, current challenges, and the role of syngas". *Combust. Sci. and Tech.,* **180**, p. 12071244.

[3] Aguiar, P., Adjiman, C., and Brandon, N., 2004. "Anode-supported intermediate temperature direct internal reforming solid oxide fuel cell. I: model-based steady-state performance". *Journal of Power Sources,* **138**(1-2), pp. 120–136.

[4] Molinelli, M., Larrain, D., Autissier, N., Ihringer, R., Sfeir, J., Badel, N., Bucheli, O., and Van herle, J., 2006. "Dynamic behaviour of SOFC short stacks". *Journal of Power Sources,* **154**(2), pp. 394–403.

[5] Pukrushpan, J., Peng, H., and Stefanopoulou, A., 2004. "Control-Oriented Modeling and Analysis for Automotive Fuel Cell Systems". *Journal of Dynamic Systems, Measurement, and Control,* **126**, p. 14.

[6] Zhang, X., Li, J., Li, G., and Feng, Z., 2006. "Development of a control-oriented model for the solid oxide fuel cell". *Journal of Power Sources,* **160**(1), pp. 258–267.

[7] Yang, Y., Wang, F., Chang, H., Ma, Y., and Weng, B., 2007. "Low power proton exchange membrane fuel cell system identification and adaptive control". *Journal of Power Sources,* **164**(2), pp. 761–771.

[8] Buchholz, M., Eswein, M., and Krebs, V., 2008. "Modelling PEM fuel cell stacks for FDI using linear subspace identification". In *IEEE International Conference on Control Applications, 2008. CCA 2008*. pp. 341–346.

[9] Ljung, L., 1999. *System identification: theory for the user*, 2nd ed. Prentice-Hall.

[10] Hsu, K., Poolla, K., and Vincent, T. L., 2008. "Identification of structured nonlinear systems". *IEEE Transactions on Automatic Control,* **58**(11), pp. 2497–2513.

[11] Zhu, H., Kee, R., Janardhanan, V., Deutschmann, O., and Goodwin, D., 2005. "Modeling elementary heterogeneous chemistry and electrochemistry in solid-oxide fuel cells". *J. Electrochem. Soc.,* **152**, pp. A2427–A2440.

[12] Kee, R., Zhu, H., and Goodwin, D., 2005. "Solid-oxide fuel cells with hydrocarbon fuels". *Proceedings of the Combustion Institute,* **30**(2), pp. 2379–2404.

[13] Soderstrom, T., and Stoica, P., 1988. System Identification. Englewood Clis.